Journal of Membrane Science 548 (2018) 194–202

Contents lists available at ScienceDirect

Journal of Membrane Science

journal homepage: www.elsevier.com/locate/memsci

Zwitterionic functionalized "cage-like" porous organic frameworks for nanofiltration membrane with high efficiency water transport channels and anti-fouling property

Chongbin Wang[a,b,c], Zhiyuan Li[a], Jianxin Chen[a,*], Yunlong Zhong[a], Yongheng Yin[b,c], Li Cao[b,c], Hong Wu[b,c]

[a] Engineering Research Center of Seawater Utilization Technology, Ministry of Education, Hebei University of Technology, Tianjin 300130, China
[b] Key Laboratory for Green Chemical Technology of Ministry of Education, School of Chemical Engineering and Technology, Tianjin University, Tianjin 300072, China
[c] Collaborative Innovation Center of Chemical Science and Engineering (Tianjin), Tianjin 300072, China

ARTICLE INFO

Keywords:
High flux, Anti-fouling, Nanofiltration composite membrane
Zwitterionic functionalized POFs
Interfacial polymerization

ABSTRACT

Nanofiltration membranes bearing high separation and anti-fouling performances represent an efficient separation technology for desalination applications. Although porous organic frameworks (POFs) are considered as a promising candidate for constructing membranes with improved water flux due to their unique advantages such as well-defined pores and tunable functionality, there is still challenge for anti-fouling property of the membranes. Zwitterions possessing balanced charge groups are very attractive for preparing anti-fouling membranes owe to their high hydration capacity. In this study, nanocomposite membranes were prepared by embedding the zwitterionic functionalized "cage-like" POFs (Z-PAF-C) into polyamide (PA) layer. The POFs blended within polymeric membranes could provide more and shorter channels for water molecules through the hybrid membranes, attributing to the novel porous structure of POFs. The zwitterionic groups derived from Z-PAF-C could enhance the hydrophilicity of membrane surface, rendering the membranes promising anti-fouling properties. The water flux of the membrane was increased distinctly from 24 L m^{-2} h^{-1} to 42.6 L m^{-2} h^{-1} under 0.2 MPa with the loading of Z-PAF-C ranged from 0 g/m^2 to 0.85 g/m^2 while the retention for Na_2SO_4 (1 g/L) was maintained at 90.6%. This study demonstrated that the introduction of the zwitterionic functionalized POFs can improve the hydrophilicity and charge negativity of membrane surface, resulting in an enhanced water flux and anti-fouling property.

1. Introduction

Currently, a rapid consumption of global water sources and increasing environmental problems lead to an urgent requirement for liquid separation processes, such as water desalination, wastewater recycling, freshwater production, etc [1–3]. Membrane-based separation technology, attributed to its relatively low investment and high efficiency, has been considered as a promising and attractive resolution to liquid separation [4–6]. Nevertheless, the trade-off effect between permeability and selectivity limits the application of conventional polymer membrane [7–10]. Hybrid membrane, which is fabricated by incorporating nanomaterials into polymer matrix, has attracted great attention due to its considerable potential to address this issue [11,12]. Several kinds of inorganic materials, including zeolite, titanium dioxide, graphene oxide and carbon nanotubes, have been explored for constructing nanostructured membranes [13–16]. However, the great challenge for existing hybrid membrane is the poor compatibility between inorganic materials and polymer matrix, leading to separation performance decline [17,18]. Besides, the inorganic materials are easy to agglomerate in polymeric matrices, which may seriously deteriorate the separation performance of membranes. In addition, membrane fouling is also a serious issue that prevents further widespread use of membranes in practical applications since foulants on the membrane surface usually results in an increase in trans-membrane pressures and a decrease in permeation fluxes [19]. Thus, novel materials with better affinity to organic polymers and excellent anti-fouling properties are earnestly demanded for fabricating a good membrane with enhanced separation performances and anti-fouling properties.

Porous organic frameworks (POFs), linked solely by strong covalent bonds, represent a burgeoning type of crystalline nanoporous materials with predesignable structure [20]. Recently, POFs in which organic building blocks form highly ordered networks, attract an increasing

* Correspondence to: School of Marine Science & Engineering, Hebei University of Technology, Tianjin 300130, PR China.
E-mail address: chjx2000@126.com (J. Chen).

https://doi.org/10.1016/j.memsci.2017.11.013
Received 3 August 2017; Received in revised form 24 October 2017; Accepted 1 November 2017
Available online 05 November 2017
0376-7388/

interest in many fields such as gas adsorption, optoelectronic and catalysis [21–24]. Due to the special properties such as tunable pore sizes, robust microporous networks and relatively low density [25,26], POFs exhibit great potential in separation field. Most importantly, because the POFs are constructed based on entire organic-organic covalent bonds, so they can be used to fabricate structurally well-formed hybrid membrane with outstanding interface compatibility. Our recent work has demonstrated that porous organic frameworks can be used as a favorable filler to increase the water flux [31]. Nevertheless, enhancing the anti-fouling property of the membranes still remains a challenge.

Zwitterions, containing equivalent cationic and anionic in the same monomer unit, has gained an increasing attention, owing to its appealing properties such as excellent antifouling property and blood compatibility [27]. The distinctive water binding ability of zwitterionic materials is benefit for improving antifouling property via forming strong hydration layer on the membrane surface [28]. An et al. reported that the membrane fabricated by incorporating zwitterionic polyelectrolyte nanoparticles exhibited an improved anti-fouling performance [11]. Zhang et al. constructed nanofiltration membranes with improved antifouling performances by embedding surface zwitterionic functionalized graphene oxide into membrane [29]. Therefore, a hybrid membrane, in which zwitterionic functionalized porous organic frameworks acted as novel building blocks, could be fabricated with improved both separation and anti-fouling performances.

In this study, novel cage-like porous aromatic frameworks (PAF-C) were synthesized successfully via copolymerizing piperazine and cyanuric chloride. Then zwitterions were grafted onto POFs through chemical grafting reaction between PAF-C and 1,3-propane sultone (1,3-PS). In the last step, thin film nanocomposite membranes were fabricated by incorporating the surface zwitterionic functionalized POFs (Z-PAF-C) into membrane via interfacial polymerization method. The novel cage-like structure of POFs were considered to be benefit for adjusting the microstructure of membranes which could enhance the separation performance of membrane. Meanwhile, the zwitterionic functionalized POFs were expected to improve the antifouling property of membranes, which was attributed to the increased hydrophilicity and electronegativity. The influence of Z-PAF-C on the micro-structure, chemical structure, hydrophilicity, surface charge properties, etc. of hybrid membranes was characterized. The effect of Z-PAF-C loading on the membrane desalination performance and the antifouling performance were investigated in detail.

2. Experiment

2.1. Materials and chemicals

Polyether sulfone (PES, E6020P) was bought from BASF Co. (Germany) and dried at 60 °C for 24 h. Poly (ethylene glycol) (PEG, MW = 2000 g/mol) and piperazine was obtained from Guangfu Fine Chemical Research Institute. The trimesoyl chloride (TMC) was supplied by Heowns Biochemical Technology Co. (Tianjin, China). Cyanuric chloride was obtained from Aladdin. N,N-dimethyl formamide (DMF), Triethylamine, n-heptane and tetrahydrofuran (THF) were purchased from Benchmark Chemical Reagent Co. (Tianjin, China).

2.2. Synthesis of cage-like POFs (PAF-C)

The cage-like POFs were synthesized via copolymerizing piperazine and cyanuric chloride using triethylamine as acid-binding agent and described as follows. Typically, 0.517 g triazine trichloride was dissolved in 100 ml THF under ice-water bath condition. Then, 0.738 g piperazine and 9 ml triethylamine were added. The mixture was heated to 66 °C for overnight after stirring at 0 °C for 4 h. After being cooled to ambient temperature, a white powder was collected by filtration. Afterwards, the crude product was washed with THF, water and ethanol for several times. The purified product was dried under vacuum at 110 °C overnight. The main pore size of voids in PAF-C was ~ 14.7 Å which was calculated by Materials Studio (MS). Fig. 1. showed the schematic illustration for the synthesis of the PAF-C.

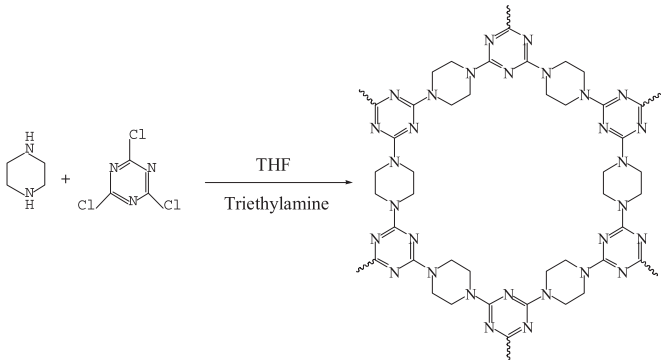

Fig. 1. The schematic illustration for the synthesis of the PAF-C.

2.3. Synthesis of the zwitterionic functionalized POFs (Z-PAF-C)

As presented in Fig. 2, the zwitterionic functionalized POFs was prepared via ring opening reaction of PAF-C with 1, 3-PS [30]. Typically, 0.2 g PAF-C powder was dispersed in 30 ml acetonitrile under stirring, then a mixture containing 1 g 1, 3-PS and 5 ml acetonitrile was added into the solution at room temperature and stirred for 10 min. Afterwards the reaction was kept stirring at 60 °C for 12 h. A white crude product was separated by centrifugation after the reaction was completed. The precipitate was washed thoroughly with acetone. Finally, the obtained Z-PAF-C was dried under vacuum at 35 °C for 12 h. Fig. 2. depicted the synthetic route and chemical structure of the Z-PAF-C.

2.4. Preparation of PA membrane

PES microporous membrane with molecular weight cut off (MWCO) above 60,000 Da was prepared as the supporting of nanofiltration membrane. The fabrication of substrate was reported in our previous work [31]. A tailored PES microporous substrate (effective area of 28.7 cm^2) was installed at the bottom of a filtration cell (model 8200, Millipore Co.) which connected with a solution reservoir and a nitrogen gas cylinder. Then 80 ml aqueous solution of PIP (1 g/L) was put into the filtration cell and drained within 20 min using the dead-end filtration system. The excess aqueous solution on the support layer surface was removed with filter papers. Afterwards, the PIP impregnated PES membrane was immersed into n-heptane solution containing 1 g/L TMC to form a polyamide thin film within certain time. Subsequently the membrane was kept in air at room temperature for 30 min. After that, the fabricated membrane was washed thoroughly with water to stop the polymerization reaction and stored in deionized water before use. The POFs modified PA (Z-PAF-C/PA) membrane was prepared according to the same procedure as above except that Z-PAF-C was dispersed to the PIP aqueous solution as addictive. Notably, the PIP aqueous solution containing POFs was treated with a probe sonicator for 30 min before filtration.

2.5. Characterizations

The surface and cross-sectional morphology of as-fabricated membranes were analyzed using field emission scanning electron microscope (FESEM, Nanosem 430). The surface topology of the prepared membranes was investigated using atomic force microscopy (AFM, CSPM5000). The chemical structure of the POFs, functionalized POFs and fabricated membranes was characterized using a FT-IR analyzer (Bruker Vertex 80 V). The hydrophilic behavior of hybrid membranes

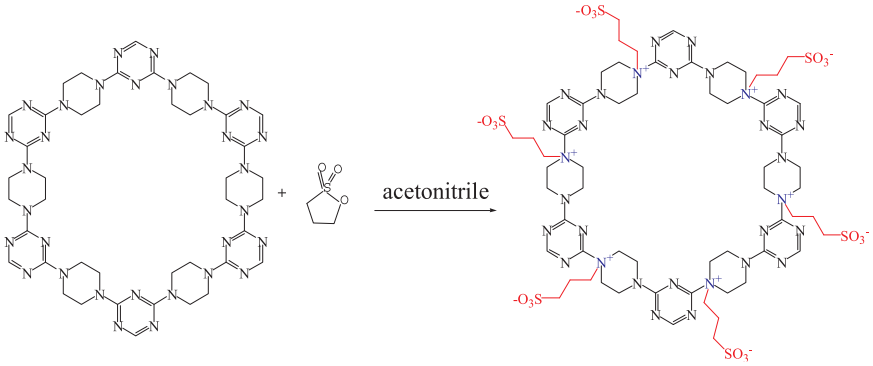

Fig. 2. The synthetic route and chemical structure of the Z-PAF-C.

surface was measured utilizing a contact angle goniometer (JC2000C Contact Angle Meter, Powereach Co.). An average value was acquired by measuring five random locations on membrane surface. The zeta potential of membrane surface was evaluated suing SurPASS Electrokinetic Analyzer (Anton Paar KG, Austria).

2.6. Desalination performance of the fabricated membranes

A dead-end stirred cell filtration system as described in Subsection 2.4 was used to study the separation properties of the prepared nanofiltration membranes. The tests of prepared membranes properties, including water flux and retention to salt, were carried out under 0.2 MPa operation pressure at room temperature. All the nanofiltration membranes were initially pretreated with deionized water at 0.25 MPa for 30 min to reach a steady permeate flux. Na_2SO_4 solution (1 g/L, 5 g/L) were used as the feed to evaluate the separation performance. The water flux (Fw, L m^{-2} h^{-1}) and retention (R%) to inorganic salt were calculated from the following Eqs. (1) and (2) respectively:

$$F_W = \frac{V}{A \times t} \quad (1)$$

where V (L) was the permeate volume, A (m^2) was the effective area of membrane and t (h) stood for the permeation time (h).

$$R = \left(1 - \frac{C_p}{C_f}\right) \times 100\% \quad (2)$$

where C_p and C_f represented salt concentration in permeate and feed solutions, respectively. All membranes were measured at least three times to obtain an average value.

2.7. Antifouling performances

The membrane antifouling experiments were carried out under 0.2 MPa at room temperature. Solutions of 1 g/L bovine serum albumin (BSA) and 1 g/L humic acid (HA) were used as model foulant for as-prepared membrane. Each membrane was pre-compacted at 0.25 MPa with pure water to obtain a stable water flux. J was the permeate flux at the beginning of experiments, J_0 stood for the permeate flux at certain time. The antifouling performance of membranes was calculated by the flux decline (J/J_0).

3. Results and discussion

3.1. Preparation of the Z-PAF-C/PA membranes

The schematic diagram of preparation process for Z-PAF-C/PA membranes was displayed in Fig. 3. The PES substrate was firstly fabricated using non-solvent-induced phase separation method. Thereafter, piperazine solution containing certain amounts of Z-PAF-C was poured onto the PES membrane surface. Finally, a polyamide layer upon PES membrane was formed by immersing the PIP impregnated substrate into n-heptane organic phase of TMC.

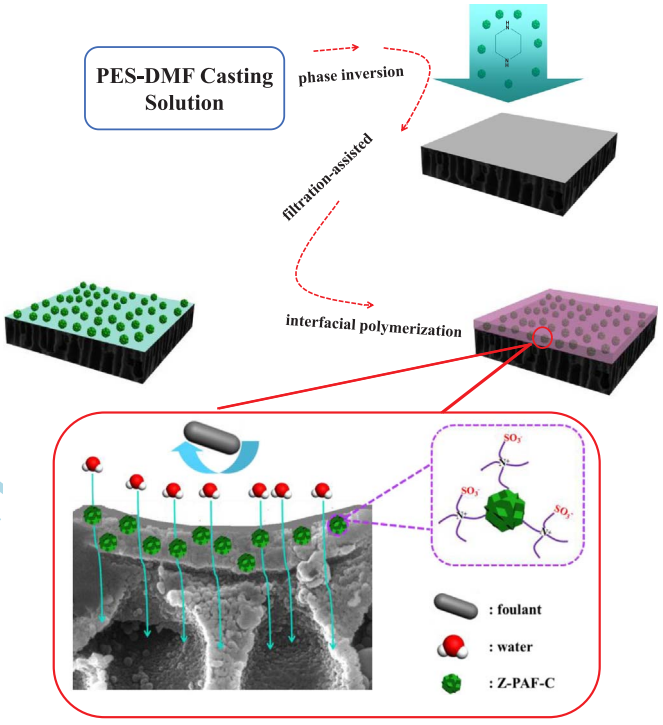

Fig. 3. The fabrication process of the Z-PAF-C/PA membrane.

3.2. Characterization of PAF-C and membranes

3.2.1. Characterization of PAF-C

SEM was used to analyze the morphology and structure of the PAF-C (Fig. 4). It was interesting to observe that the novel nanomaterial was actually cage-like entities with a uniform morphology and a highly ordered structure. As can be seen from Fig. 4a, the PAF-C, with a diameter about 240 nm, consisted of large amount 2D sheets. As shown in Fig. 4b and c, a large number of pores could be observed in the PAF-C which might be act as channels to allow water molecular pass in membrane.

The chemical structure of the PAF-C and Z-PAF-C was analyzed by FT-IR (Fig. 5a). The peaks located at 2900 cm^{-1} and 1500 cm^{-1} in the spectra were ascribed to the stretching vibration of alkane C-H from piperazine and stretching vibration of the aromatic C-N from triazine ring, respectively. Notably, the characteristic peak at 850 cm^{-1} assigned to the stretching vibration of C-Cl in the cyanuric chloride disappeared in the spectra of PAF-C and Z-PAF-C, indicating that chlorine atoms were substituted completely. Compared with PAF-C, two new peaks at 1230 cm^{-1} and 1030 cm^{-1} appeared in the spectra of Z-PAF-C were attributed to the stretching vibration of S=O, revealing the

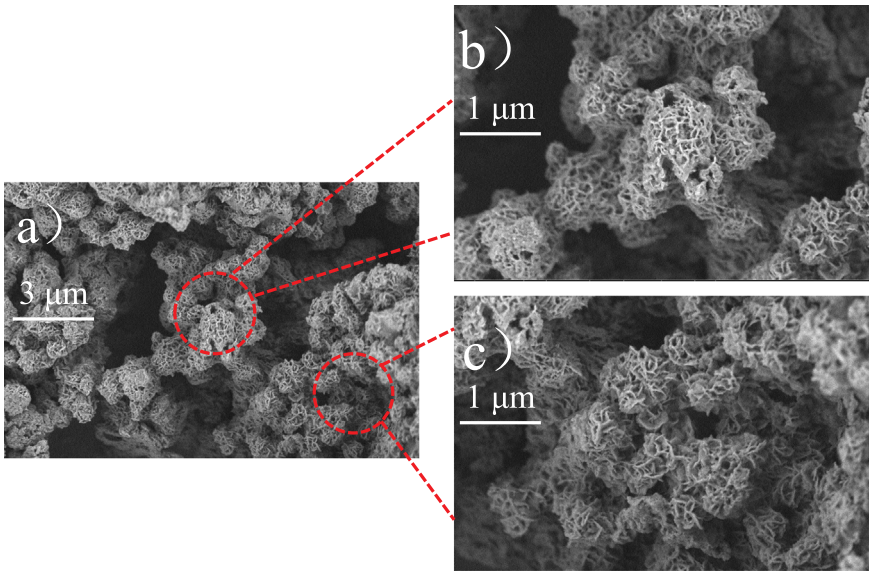

Fig. 4. SEM images of PAF-C.

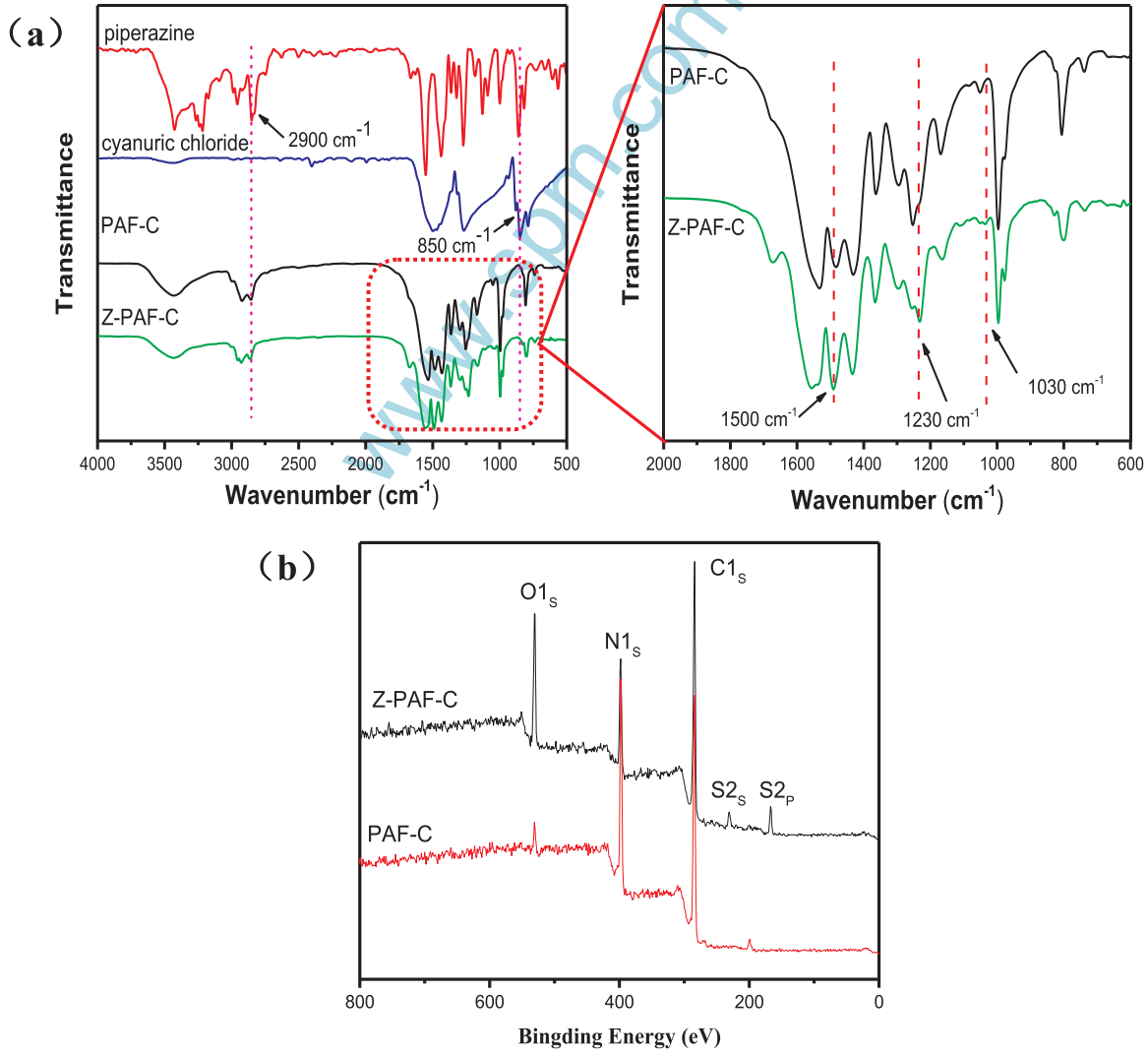

Fig. 5. a) FTIR spectra of piperazine, cyanuric chloride, PAF-C and Z-PAF-C, b) XPS spectra of PAF-C and Z-PAF-C.

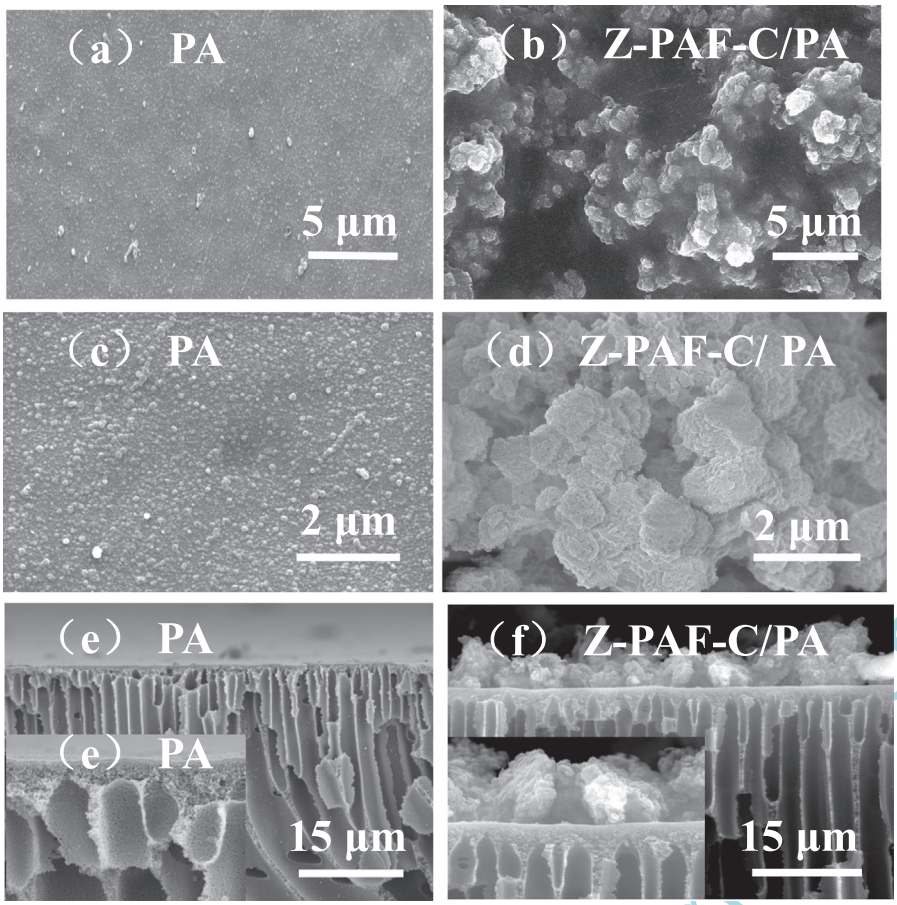

Fig. 6. SEM images of the surface and cross section of prepared membranes, a, c, e) PA and b, d, f) Z-PAF-C/PA.

successful zwitterionic functionalization. The zwitterionization procedure was further confirmed by XPS spectra as shown in Fig. 5b. The oxygen content in the Z-PAF-C spectra evidently increased from 3.5% to 14.58% compared to the PAF-C spectra, and the new peaks at 168 eV and 230 eV corresponded to the sulfur element from sulfonate. Both the above evidence confirmed the existence of zwitterion in the Z-PAF-C.

3.2.2. Characterization of membranes

Fig. 6. depicted the surface and cross-sections microstructure of the as-prepared composite membranes. It was obvious to find the influence of incorporating Z-PAF-C into PA layer, the top surface of membrane produced with 0.85 g/m^2 loading of particles was rougher and looser compared with the pristine PA membrane. The Z-PAF-C was uniformly distributed and almost overspread on the top of membrane surface. The spherical shape of Z-PAF-C was still kept, implying that the physical structure of Z-PAF-C was maintained, which was benefit for improvement of water flux. Fig. 6e and f depicted cross-section morphology of prepared membranes respectively. Both of them were composed of a finger-like porous layer and a dense layer. The thickness of the PA layer fabricated with Z-PAF-C was around 6 μm which indicated that the morphology was considerably affected by embedding Z-PAF-C. In addition, there were no distinct flaws on the surface of Z-PAF-C modified composite membrane, indicating good compatibility between organic fillers and polymer matrix. The chemical bonds formed between the -NH- groups of Z-PAF-C and the -COCl groups of trimesoyl chloride in interfacial polymerization process was beneficial to membrane stability [32].

The top morphological structure of pristine PA membrane and Z-PAF-C/PA membrane fabricated with 0.85 g/m^2 additions loading were further visualized by AFM, the morphology images were shown in Fig. 7. Clearly, a typical “ridge-and-valley” structure was observed in these membranes surface. Compared with the pristine PA membrane, the hybrid membrane possessed a rougher surface based on the value of root mean squared (RMS) roughness which was previously proved by SEM images. The increase of roughness after incorporating the Z-PAF-C into PA layer could be attributed to the heterogeneous dispersion of additions in the membrane.

The surface chemical structure changes for prepared membrane were investigated by ATR-IR and the spectra were displayed in Fig. 8. In comparison with the PES membrane, a new characteristic peak at 1628 cm^{-1}, which was ascribed to the carbonyl stretching vibration of amide group, appeared in the spectrum of PA membrane, indicating successful interfacial polymerization reaction. The intensity of the typical peaks originating from PES distinctly declined for the Z-PAF-C/PA membrane. In the meantime, two new characteristic peaks at 1535 cm^{-1} and 1438 cm^{-1} were observed, which were attributed to the absorption bands of the triazine ring from Z-PAF-C. The results revealed that the Z-PAF-C was embedded into polyamide structure during interfacial polymerization process.

Surface hydrophilicity plays a vital role for nanofiltration membrane in desalination applications because better affinity to water is prone to higher water-capture ability, which in turn could bring about greater water flux and antifouling property [33]. Here, the surface hydrophilicity of PA membrane and hybrid membranes fabricated with 0.85 g/m^2 additions loading were investigated by the contact angle measurements. As shown in Fig. 9, the value of contact angle for the membrane prepared with no additives embedded was higher than that of membrane containing PAF-C without zwitterionic functionalized which could be attributed to the increased roughness of membranes [34,35]. The membrane constructed with zwitterionic functionalized PAF-C exhibited the best surface hydrophilicity among the prepared membranes. This phenomenon can be explained by the presence of zwitterionic groups in the Z-PAF-C. The zwitterionic groups were capable of capturing large amount of “free water”, resulting in the

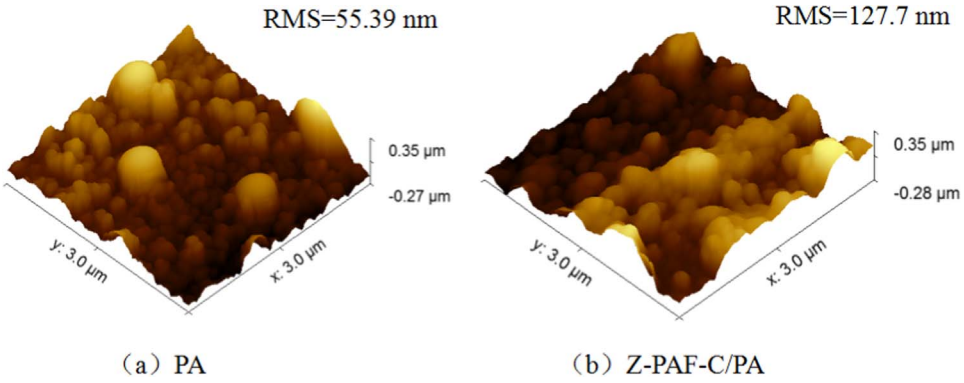

Fig. 7. AFM images of PA and Z-PAF-C/PA membrane.

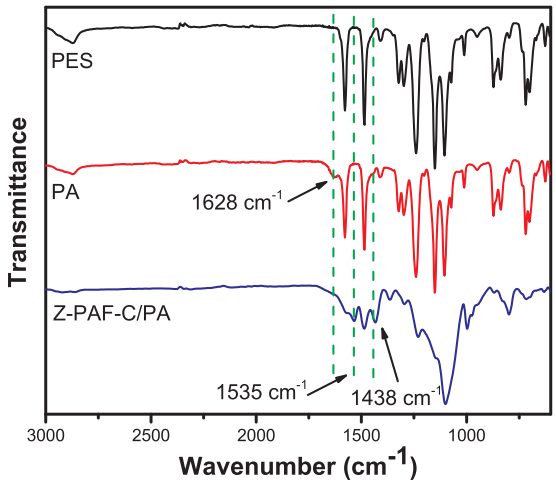

Fig. 8. FTIR spectra of PES, PA and Z-PAF-C/PA.

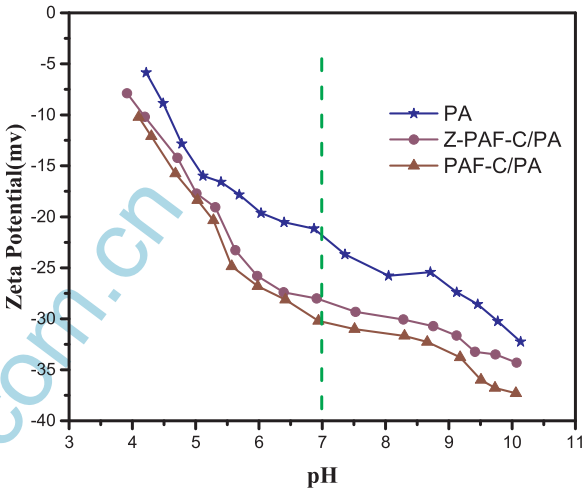

Fig. 10. Zeta potential of PA, Z-PAF-C/PA and PAF-C/PA membrane.

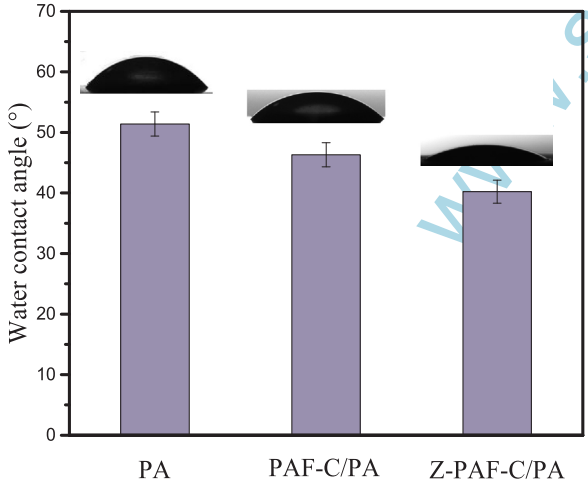

Fig. 9. Contact angles of PA, PAF-C/PA and Z-PAF-C/PA membrane.

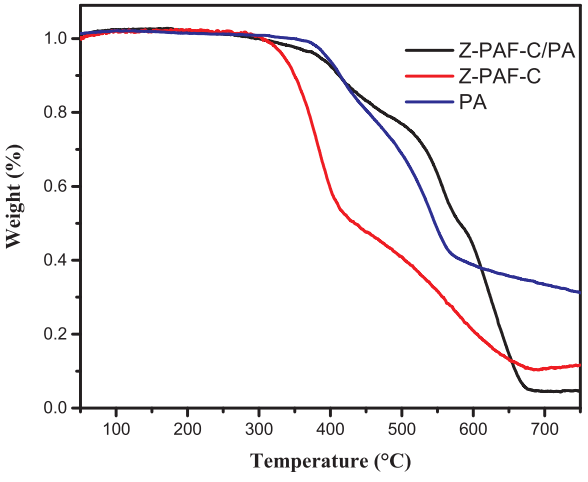

Fig. 11. TGA curves of PA, Z-PAF-C/PA membrane and Z-PAF-C.

formation of tightly bound water layer adjacent to the membranes surface [33,36].

The surface charge properties of the membranes were further confirmed by zeta potential test, which was one of the most important factors that influenced the separation and antifouling properties of NF membranes [37]. As shown in Fig. 10, both the pristine PA membrane and hybrid membrane produced with 0.85 g/m^2 additions loading possessed a negative zeta potential and the intensity of surface charge became increasingly lower with the incorporation of Z-PAF-C or PAF-C into PA layer. The explanation was that more carboxylic acid groups were generated from the hydrolysis of unreacted acid chloride groups [38]. Notably, the membrane prepared containing PAF-C without zwitterionic functionalized exhibited a higher electronegative zeta potential than that of membrane fabricated with Z-PAF-C which could be attributed to the shadowing effect from the zwitterionic functionalized polymer. Compared with pristine PA membrane, the more electronegative property for hybrid membrane had a significantly positive affect for separating charged solutes and salts due to the donnan effect [29].

The thermal stability of Z-PAF-C nano-particles, pristine PA membrane and hybrid membrane produced with 0.85 g/m^2 Z-PAF-C loading were investigated by TGA and the results were exhibited in Fig. 11. The

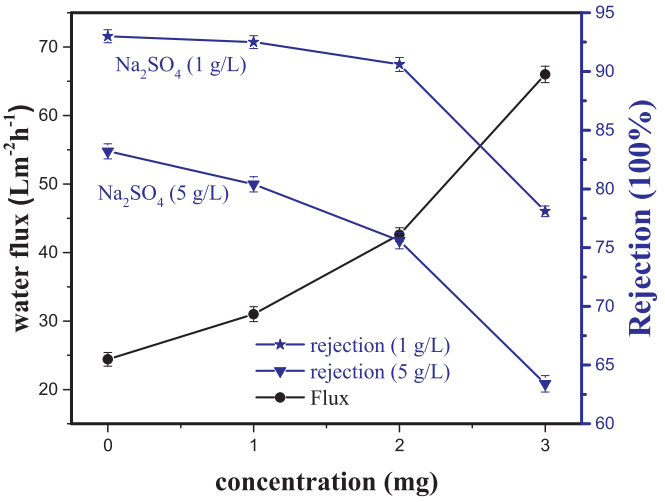

Fig. 12. Influence of Z-PAF-C loading on the membrane properties.

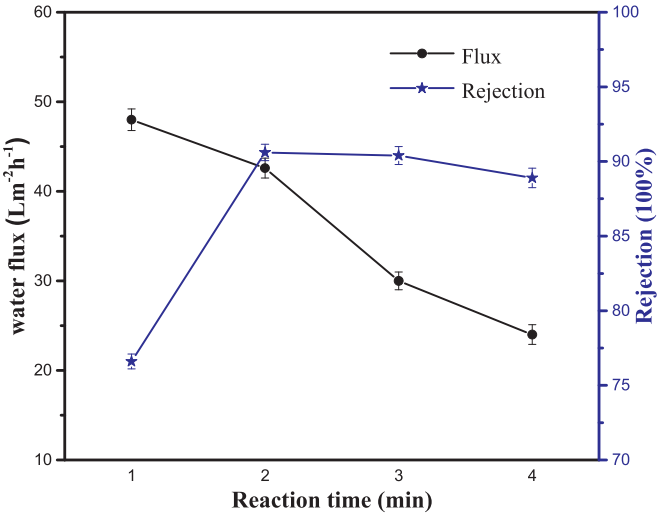

Fig. 13. Influence of reaction time on the membrane properties.

weight loss of Z-PAF-C was negligible below 320 °C, proving that the thermal stability of the additions was adequate for the practical nanofiltration application. Both the Z-PAF-C/PA membrane and the pristine PA membranes presented excellent thermal stability below 350 °C. The weight loss for both membranes in the range from 420 °C to 620 °C was similar, which was mainly due to the degradation of PA layer and PES skeleton. However, the residue for the Z-PAF-C/PA membrane in this weight loss stage was higher than that for PA membrane, indicating that the incorporation of Z-PAF-C changed the interaction of polymer chains. Besides, it was assumed that part of polymer chain entered into the pores of POFs which could also result in the difference of residue between the hybrid membrane and pristine PA membrane. The residue for the hybrid membrane in the range of 620–750 °C was lower than that for the pristine PA membrane which was attributed to the degradation of Z-PAF-C in the membrane.

3.3. Separation performances of the Z-PAF-C/PA membranes

3.3.1. Effects of Z-PAF-C loading on membrane performances

The performances of the Z-PAF-C/PA hybrid membranes fabricated with different Z-PAF-C loading were investigated at room temperature with pure water and Na_2SO_4 solution. The interfacial polymerization time was two minutes and the results were presented in Fig. 12. The water flux of as-prepared hybrid membranes was markedly improved by further increasing the Z-PAF-C loading. The water flux was increased distinctly from 24 L m^{-2} h^{-1} to 66 L m^{-2} h^{-1} with the loading of Z-PAF-C ranged from 0 g/m^2 to 1 g/m^2. The results could be owe to the following factors. First of all, the surface hydrophilicity of the Z-PAF-C/PA membranes was enhanced evidently by the addition of Z-PAF-C. The zwitterionic groups derived from Z-PAF-C could capture large mount water molecules to form water layer upon hybrid membrane surface, promoting water to pass through channels in membranes with lower resistance [29]. Also, the enlargement of membrane surface resulting from the incorporation of Z-PAF-C produced a significant impact in enhancing the water flux of hybrid membrane. The increase of effective membrane area provided more opportunity to allow substance transport. In addition, the interaction and space of the polyamide macromolecules were influenced by introducing Z-PAF-C into the PA layer, making the hybrid membrane structure much looser with lower density. The loose membrane structure was assumed to be benefit for the improvement of water flux. Besides, the interfacial space between the Z-PAF-C and polymer chains played a positive influence on the water flux [11]. The inherent hole in the Z-PAF-C was a factor in influencing the water flux of hybrid membrane that could not be ignored. The special physical structure of the Z-PAF-C could likely provide chance to form more and shorter water channels in the membrane, increasing the water flux significantly [31].

The separation property to Na_2SO_4 (1 g/L) of the composite membranes was slightly changed by increasing the Z-PAF-C loading from 0 g/m^2 to 0.85 g/m^2. This could be explained by that the structure of membranes became loose after the insertion of Z-PAF-C into PA layer. The separation property of the prepared membranes was little influenced at a small amount of Z-PAF-C loading. However, the rejection for salt of the hybrid membrane decreased dramatically from 90.6% to 78.1% with the loading of Z-PAF-C ranged from 0.85 g/m^2 to 1 g/m^2. The sharply decline of separation property was attributed to that the Z-PAF-C particles was likely prone to agglomerate, enlarging the interfacial gaps between the Z-PAF-C and polymer chains. Although the flaws might bring about an increase in water flux, there were a negative influence in maintaining rejection to salt [11]. Clearly, the membrane produced with 0.85 g/m^2 Z-PAF-C loading exhibited the best membrane performances which possessed a 42.6 L m^{-2} h^{-1} water flux while the retention for Na_2SO_4 (1 g/L) was maintained above 90%. Notably, compared with the pristine PA membrane, the as-prepared hybrid membrane exhibited more intensity of surface electronegativity which was benefit for enhancing the electrostatic repulsion between SO_4^{2-} anions and membrane surface, improving the separation properties of membranes.

3.3.2. Effects of reaction time on membrane performances

The performances of the hybrid membranes produced with 0.85 g/m^2 Z-PAF-C loading were investigated at room temperature with different interfacial polymerization time and the results were depicted in Fig. 13. The water flux decreased apparently as the reaction time increased which may be explained by the density of PA layer. The degree of interfacial polymerization further improved as extending the reaction time. The membrane structure became more compact, enhancing resistance of the water molecules through hybrid membrane.

The rejection to Na_2SO_4 (1 g/L) increased evidently from 76.6% to 90.6% with the reaction time ranged from 1 min to 2 min. This can be simply explained by the mechanism of size exclusion. The fabricated PA layer was not integrated at the beginning of reaction, resulting in a low retention to salt. However, the separation performance of membranes was stable and even declined slightly with further increasing reaction time. This was because that the self-limiting phenomenon occurred. The structure of Z-PAF-C/PA membrane was loose in the initial stage of reaction and the interfacial space between the Z-PAF-C and polymer chains played minor affect in separation property [29]. The gaps acted as the channels of salt solution could not be ignored with increasing reaction time which could bring about the decrease in separation

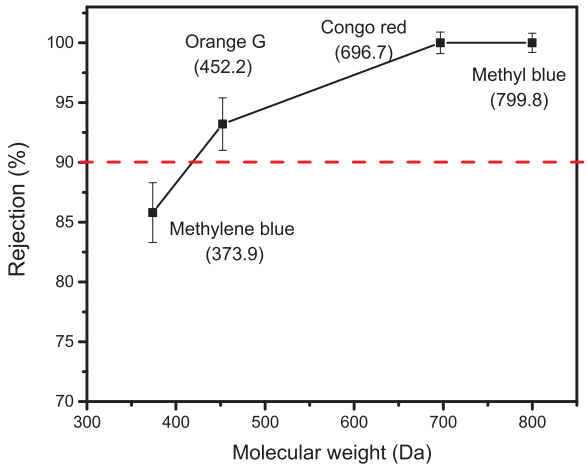

Fig. 14. The MWCO of the hybrid membrane fabricated with 0.85 g/m^2 loading.

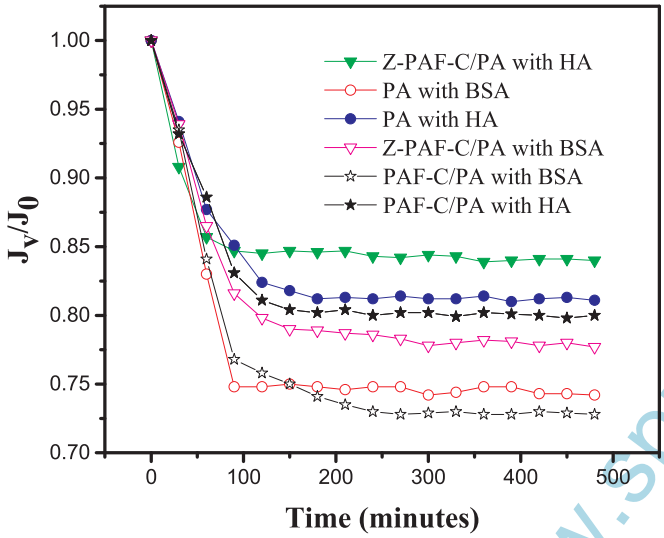

Fig. 15. Fouling characterization of PA, PAF-C/PA and Z-PAF-C/PA membranes with HA and BSA aqueous solution.

performance.

3.3.3. The rejection to dyes for the hybrid membrane

The separation performance of the hybrid membranes fabricated with 0.85 g/m^2 additions loading was also evaluated by molecular weight cut-off (MWCO). The MWCO value was calculated using dyes that were rejected by the hybrid membrane to 90% [39]. Four kinds of dyes including Methylene blue (MW = 373.9 g/mol), Orange G (MW = 452.4 g/mol), Congo red (MW = 696.7 g/mol) and Methyl blue (MW = 799.8 g/mol) were used as model solutes. Fig. 14 depicted the rejections of the hybrid membrane to dyes. The retention of the membrane was 85.8%, 93.2%, 100% and 100% for Methylene blue, Orange G and Congo red and Methyl blue, respectively. The MWCO values of Z-PAF-C/PA membrane was around 418 Da.

3.4. Antifouling performances of membranes

In order to investigate the anti-fouling performances of Z-PAF-C/PA nano-composite membranes, the changes of membranes permeate flux were investigated. BSA and HA were selected as protein model and natural organic matter model, respectively. To further confirm the antifouling property, membranes containing PAF-C without zwitterionic functionalized (PAF-C/PA) were also fabricated for comparison and Fig. 15 depicted the experimental results. The permeate flux for each membrane decreased dramatically, attributing to the concentration polarization and accumulation of foulants on the membrane surface at first stage. Then the water flux reached stability due to the balance of desorption and adsorption for foulants. However, the total flux decline ratio for the membrane fabricated with no additives incorporated was slightly lower than that of membrane containing PAF-C without zwitterionic functionalized. It was assumed that the incorporation of PAF-C into membrane increased the wave of the membrane outer surface as proved by AFM images, resulting in accumulation of foulants on the membrane. Clearly, the membrane fabricated with zwitterionic functionalized PAF-C exhibited the best anti-fouling properties among the prepared membranes, this could be explained by three possible mechanisms. First of all, the composite membrane embedded with Z-PAF-C possessed higher hydrophilic surface according to the contact angle measurement [39]. The hydrophilic surface would weaken interaction between foulants and membrane surface, preventing the absorption of protein and organic matter. Secondly, the higher anti-fouling properties of hybrid membrane were due to the more electronegative membrane surface confirmed by the zeta potential measurement. The reason for this was that the foulants used in the nanofiltration process also were negative charged. The improved electrostatic repulsion interaction between foulants and the surface of hybrid membrane endowed the prepared membrane higher anti-fouling performances to a certain extent [40]. Thirdly, the zwitterionic groups in the Z-PAF-C could form a water layer adjacent to the hybrid membrane surface, preventing the attachment of foulants to the membrane surface. Although there was negative influence on the improvement of membrane anti-fouling properties such as the increased waves of membranes surface, it was probably not the crucial factor to affect the membrane anti-fouling performances. In summary, the improved surface hydrophilicity, enhanced surface charge negativity and the formation of “free water” layer strengthened the anti-fouling properties of Z-PAF-C/PA hybrid membrane.

4. Conclusions

A novel cage-like POFs was firstly synthesized and then surface zwitterionization of POFs was prepared successfully by the ring opening reaction. The nanocomposite membranes were fabricated by introducing the zwitterionic functionalized POFs into polyamide layer during interfacial polymerization process. The special porous structure combined with fascinating surface zwitterionization of POFs strengthened the filtration process. The water flux of the membrane produced with 0.85 g/m^2 Z-PAF-C loading reached up to 42.6 L m^{-2} h^{-1} under 0.2 MPa while the retention for Na_2SO_4 (1 g/L) maintained at 90.6%. The hybrid membrane prepared with zwitterionic functionalized POFs also exhibited improved anti-fouling properties compared with the pristine PA membrane and the membrane containing POFs with no zwitterionic functionalized. Incorporating zwitterionic functionalized POFs into membrane might pave the way to prepare membranes with high water flux and anti-fouling properties for water treatment applications.

Acknowledgement

The research was financially supported by the National Natural Science Foundation of China (21476059, 21576189 and 21276063), Hebei Science and Technology Support Program (16273101D), the Key Project of Natural Science Foundation of Tianjin (16JCZDJC36500).

References

[1] R. van Reis, A. Zydney, Bioprocess membrane technology, J. Membr. Sci. 297 (2007) 16–50.
[2] L.S. White, Development of large-scale applications in organic solvent nanofiltration and pervaporation for chemical and refining processes, J. Membr. Sci. 286

(2006) 26–35.
[3] A. Asatekin, A. Menniti, S. Kang, M. Elimelech, E. Morgenroth, A.M. Mayes, Antifouling nanofiltration membranes for membrane bioreactors from self-assembling graft copolymers, J. Membr. Sci. 285 (2006) 81–89.
[4] H.M. Hegab, A. ElMekawy, T.G. Barclay, A. Michelmore, L. Zou, C.P. Saint, M. Ginic-Markovic, Fine-tuning the surface of forward osmosis membranes via grafting graphene oxide: performance patterns and biofouling propensity, ACS Appl. Mater. Interfaces 7 (2015) 18004–18016.
[5] R. Shukla, M. Cheryan, Performance of ultrafiltration membranes in ethanol-water solutions: effect of membrane conditioning, J. Membr. Sci. 198 (2002) 75–85.
[6] D.L. Gin, R.D. Noble, Designing the next generation of chemical separation membranes, Science (2011) 674–676.
[7] B.D. Freeman, Basis of permeability/selectivity tradeoff relations in polymeric gas separation membranes, Macromolecules 32 (1999) 375–380.
[8] Z. Lai, G. Bonilla, I. Diaz, J.G. Nery, K. Sujaoti, M.A. Amat, E. Kokkoli, O. Terasaki, R.W. Thompson, M. Tsapatsis, G. Dionisios, Microstructural optimization of a zeolite membrane for organic vapor separation, Science 300 (2003) 456–460.
[9] Y.X. Hu, J. Wei, Y. Liang, H.C. Zhang, X.W. Zhang, W. Shen, H.T. Wang, Zeolitic imidazolate framework/graphene oxide hybrid nanosheets as seeds for the growth of ultrathin molecular sieving membranes, Angew. Chem. Int. Ed. 55 (2016) 2048–2052.
[10] M.A. Shannon, P.W. Bohn, M. Elimelech, J.G. Georgiadis, B.J. Marinas, A.M. Mayes, Science and technology for water purification in the coming decades, Nature 452 (2008) 301–310.
[11] Y.L. Ji, Q.F. An, Y.S. Guo, W.S. Hung, K.R. Lee, C.J. Gao, Bio-inspired fabrication of high perm-selectivity and anti-fouling membranes based on zwitterionic polyelectrolyte nanoparticles, J. Mater. Chem. A 4 (2016) 4224–4231.
[12] S. Bolisetty, R. Mezzenga, Amyloid-carbon hybrid membranes for universal water purification, Nat. Nanotechnol. 11 (2016) 365–371.
[13] K. Vanherck, G. Koeckelberghs, I.F.J. Vankelecom, Crosslinking polyimides for membrane applications: a review, Prog. Polym. Sci. 38 (2013) 874–896.
[14] H.S. Lee, S.J. Im, J.H. Kim, H.J. Kim, J.P. Kim, B.R. Min, Polyamide thin-film nanofiltration membranes containing TiO_2 nanoparticles, Desalination 219 (2008) 48–56.
[15] J. Shen, G.P. Liu, K. Huang, Z.Y. Chu, W.Q. Jin, N.P. Xu, Subnanometer two-dimensional graphene oxide channels for ultrafast gas sieving, ACS Nano 10 (2016) 3398–3409.
[16] S. Bano, A. Mahmood, S.J. Kim, K.H. Lee, Graphene oxide modified polyamide nanofiltration membrane with improved flux and antifouling properties, J. Mater. Chem. A 3 (2015) 2065–2071.
[17] H. Vinh-Thang, S. Kaliaguine, Predictive models for mixed-matrix membrane performance: a review, Chem. Rev. 113 (2013) 4980–5028.
[18] M.T.M. Pendergast, E.M.V. Hoek, A review of water treatment membrane nanotechnologies, Energy Environ. Sci. 4 (2011) 1946–1971.
[19] D. Rana, T. Matsuura, Surface modifications for antifouling membranes, Chem. Rev. 110 (2010) 2448–2471.
[20] A.P. Cote, A.I. Benin, N.W. Ockwig, M. O'Keeffe, A.J. Matzger, O.M. Yaghi, Porous, crystalline, covalent organic frameworks, Science 310 (2005) 1166–1170.
[21] S.Y. Ding, J. Gao J, Q. Wang, Y. Zhang, W.G. Song, C.Y. Su, W. Wang, Construction of covalent organic framework for catalysis: Pd/COF-LZU1 in Suzuki-Miyaura coupling reaction, J. Am. Chem. Soc. 133 (2011) 19816–19822.
[22] F. Xu, H. Xu, X. Chen, D.C. Wu, Y. Wu, H. Liu, C. Gu, R.W. Fu, D.L. Jiang, Radical covalent organic frameworks: a general strategy to immobilize open-accessible polyradicals for high-performance capacitive energy storage, Angew. Chem. Int. Ed. 54 (2015) 6814–6818.
[23] J.W. Colson, A.R. Woll, A. Mukherjee, M.P. Levendorf, E.L. Spitler, V.B. Shields, M.G. Spencer, J. Park, W.R. Dichtel, Oriented 2D covalent organic framework thin films on single-layer graphene, Science 332 (2011) 228–231.
[24] H.Y. Zhao, Z. Jin, H.M. Su, X.F. Jing, F.X. Sun, G.S. Zhu, Targeted synthesis of a 2D ordered porous organic framework for drug release, Chem. Commun. 47 (2011) 6389–6391.
[25] M. Shan, B. Seoane, E. Rozhko, A. Dikhtiarenko, G. Clet, F. Kapteijn, J. Gascon, Azine-linked Covalent Organic Framework (COF)-based mixed-matrix membranes for CO_2/CH_4 separation, Chem.-Eur. J. 22 (2016) 14467–14470.
[26] S. Kandambeth, B.P. Biswal, H.D. Chaudhari, K.C. Rout, H. Kunjattu, S. Mitra, S. Karak, A. Das, R. Banerjee, Selective molecular sieving in self-standing porous covalent-organic-framework membranes, Adv. Mater. 29 (2017).
[27] Y. Chang, Y.J. Shih, C.J. Lai, H.H. Kung, S.Y. Jiang, Blood-inert surfaces via ion-pair anchoring of zwitterionic copolymer brushes in human whole blood, Adv. Funct. Mater. 23 (2013) 1100–1110.
[28] L. Mi, S.Y. Jiang, Integrated antimicrobial and nonfouling zwitterionic polymers, Angew. Chem. Int. Ed. 53 (2014) 1746–1754.
[29] J.Y. Zhu, M.M. Tian, J.W. Hou, J. Wang, J.Y. Lin, Y.T. Zhang, J.D. Liu, B. Van, der Bruggen, Surface zwitterionic functionalized graphene oxide for a novel loose nanofiltration membrane, J. Mater. Chem. A 4 (2016) 1980–1990.
[30] L. Chen, Y. Honma, T. Mizutani, D.J. Liaw, J.P. Gong, Y. Osada, Effects of polyelectrolyte complexation on the UCST of zwitterionic polymer, Polymer 41 (2000) 141–147.
[31] C.B. Wang, Z.Y. Li, J.X. Chen, Z. Li, Y.H. Yin, L. Cao, Y.L. Zhong, H. Wu, Covalent organic framework modified polyamide nanofiltration membrane with enhanced performance for desalination, J. Membr. Sci. 523 (2017) 273–281.
[32] H.Q. Wu, B.B. Tang, P.Y. Wu, Optimizing polyamide thin film composite membrane covalently bonded with modified mesoporous silica nanoparticles, J. Membr. Sci. 428 (2013) 341–348.
[33] H. Kitano, K. Sudo, K. Ichikawa, M. Ide, K. Ishihara, Raman spectroscopic study on the structure of water in aqueous polyelectrolyte solutions, J. Phys. Chem. B 104 (2000) 11425–11429.
[34] Z.Z.G. Wang, R. Novel, membrane surface modification to enhance anti-oil fouling property for membrane distillation application, J. Membr. Sci. 447 (2013) 26–35.
[35] M.Y. Wu, T.Y. Ma, Y.L. Su, H. Wu, X.D. You, Z.Y. Jiang, R. Kasher, Fabrication of composite nanofiltration membrane by incorporating attapulgite nanorods during interfacial polymerization for high water flux and antifouling property, J. Membr. Sci. (2017).
[36] Y.L. Ji, Q.F. An, Q. Zhao, W.D. Sun, K.R. Lee, H.L. Chen, C.J. Gao, Novel composite nanofiltration membranes containing zwitterions with high permeate flux and improved anti-fouling performance, J. Membr. Sci. 390–391 (2012) 243–253.
[37] J.M.M. Peeters, J.P. Boom, M.H.V. Mulder, H. Strathmann, Retention measurements of nanofiltration membranes with electrolyte solutions, J. Membr. Sci. 145 (1998) 199–209.
[38] Q.F. An, W.D. Sun, Q. Zhao, Y.L. Ji, C.J. Gao, Study on a novel nanofiltration membrane prepared by interfacial polymerization with zwitterionic amine monomers, J. Membr. Sci. 431 (2013) 171–179.
[39] Y.F. Li, Y.L. Su, X.T. Zhao, X. He, R.N. Zhang, J.J. Zhao, X.C. Fan, Z.Y. Jiang, Antifouling, high-flux nanofiltration membranes enabled by dual functional polydopamine, ACS Appl. Mater. Interfaces 6 (2014) 5548–5557.
[40] G.H.W.W.R. Gombotz, T.A. Horbett, A.S. Hoffman, Protein adsorption to poly (ethylene oxide) surfaces, J. Biomed. Mater. Res 25 (1991) 1547–1562.